

Photoelectron spectroscopy of group IV heavy metal dimers: Sn_2^- , Pb_2^- , and SnPb^-

Joe Ho, Mark L. Polak, and W. C. Lineberger

Department of Chemistry and Biochemistry, University of Colorado, and Joint Institute for Laboratory Astrophysics, University of Colorado and National Institute of Standards and Technology, Boulder, Colorado 80309-0440

(Received 2 August 1991; accepted 19 September 1991)

Negative ion photoelectron spectra of Sn_2^- , SnPb^- , and Pb_2^- are presented for electron binding energies up to 3.35 eV. Each spectrum exhibits multiple electronic bands, most of which contain resolved vibrational structure. Franck-Condon analyses yield spectroscopic parameters (r_e , ω_e , and T_e) for the anion ground states and the neutral excited states. Adiabatic electron affinities are determined to be: $EA(\text{Sn}_2) = 1.962 \pm 0.010$ eV, $EA(\text{Pb}_2) = 1.366 \pm 0.010$ eV, and $EA(\text{SnPb}) = 1.569 \pm 0.008$ eV. The anion dissociation energies $D_0(\text{Sn}_2^-)$ and $D_0(\text{Pb}_2^-)$ are derived from the electron affinities and the neutral dissociation energies. For SnPb^- , the dissociation energy difference $D_0(\text{SnPb}^-) - D_0(\text{SnPb})$ is precisely measured. Based on the present data, previous experiments and *ab initio* calculations, we assign most of the observed bands to the corresponding neutral low-lying electronic states.

I. INTRODUCTION

The group IV heavy metal dimers Sn_2 and Pb_2 have attracted extensive attention due to their interesting electronic properties and potential practical applications.¹ These dimers have four *s* and four *p* valence electrons, and bonding in these molecules mainly arises from open *p* shells. In addition, spin-orbit effects are expected to be important for these heavy diatomic systems. Abundant spectroscopic data on Sn_2 and Pb_2 have been obtained from various studies; however, the available information concerning the low-lying electronic excited states, anionic electronic ground states, and the nature of the metal-metal bond of these dimers is far from complete.

In previous experimental studies of Sn_2 and Pb_2 by Bondybey and co-workers,²⁻⁷ Nixon and co-workers,^{8,9} and several other groups,¹⁰ electronic spectra of Sn_2 and Pb_2 were obtained both using matrix isolation and in the gas phase. The ground states for both Sn_2 and Pb_2 have been determined¹ to be $X^3\Sigma_g^-(0_g^+)$. The strongest absorption transition for Sn_2 has been ascribed⁸ to the $C(0_u^+) \rightarrow X(0_g^+)$ system at $18\,223\text{ cm}^{-1}$. In addition, an emission system in the $12\,000\text{--}14\,000\text{ cm}^{-1}$ region was interpreted as terminating in a state $3000\text{--}5000\text{ cm}^{-1}$ above the ground state. No other Sn_2 states have been observed below 2 eV, although several low-lying electronic states are expected¹ to exist in this region. The Sn_2 dissociation energy was determined to be $15\,330 \pm 25\text{ cm}^{-1}$ (1.901 ± 0.003 eV) using laser-induced fluorescence spectroscopy.⁷ Spectroscopic studies of Pb_2 show at least six excited electronic states within $20\,000\text{ cm}^{-1}$ of the ground state.³ Two transitions, $C(0_u^+) \rightarrow X(0_g^+)$ and $F(0_u^+) \rightarrow X(0_g^+)$, are found to dominate the emission and absorption spectra. All observed excited states lie more than $12\,000\text{ cm}^{-1}$ above the ground state, except for state *A* which lies $<5500\text{ cm}^{-1}$ above the ground state.³ The best value for the Pb_2 dissociation energy, 0.86 ± 0.01 eV, was

measured utilizing mass spectrometric studies of high temperature equilibria.¹¹

Sn_2 and Pb_2 have been investigated theoretically at a variety of levels. Balasubramanian and Pitzer¹² carried out self-consistent-field (SCF) and relativistic configuration interaction (RCI) calculations. The calculations include spin-orbit coupling, and predict the properties of 10 of the low-lying electronic states of Sn_2 and Pb_2 within $10\,000\text{ cm}^{-1}$ (Sn_2) and $16\,000\text{ cm}^{-1}$ (Pb_2) of the ground state. Their work was a pioneering study, because it was the first detailed quantum chemical treatment of relativistic effects for systems containing more than one heavy atom. However, most of the predicted low-lying states have not been observed experimentally prior to this work. Pacchioni¹³ calculated the properties of the low-lying electronic states of Sn_2 and Pb_2 using semiempirical pseudopotentials and a multireference configuration interaction (MRDCI) method. Recently, Andzelm *et al.*¹⁴ calculated the spectroscopic constants of the ground and excited states of group IV dimers (Si_2 , Ge_2 , Sn_2 , SiGe , SiSn , and GeSn) with the local-spin-density (LSD) model potential method. Their results provide comparison between homonuclear and heteronuclear dimers. To our knowledge, no experimental or theoretical investigations have been performed on SnPb^- or SnPb .

A major advantage of negative ion photoelectron spectroscopy over optical spectroscopy for metal cluster studies is that the transition selection rules are less restrictive,^{15,16} and most of the neutral low-lying electronic states are directly accessible from the corresponding anion ground state. Studies of Sn_2 and Pb_2 using laser photoelectron spectroscopy can essentially map out the low-lying electronic states of these species. Recently, Ganteför *et al.*¹⁷ reported photoelectron spectra of Sn_n^- and Pb_n^- ($n = 2\text{--}20$). Their principal results were determination of the electron affinities for Sn_n and Pb_n as a function of cluster size. However, they provided no detailed assignments of the electronic states for

the metal dimers (Sn_2 and Pb_2).

In this work, we present the 351 nm photoelectron spectra of Sn_2^- , Pb_2^- , and SnPb^- . All three spectra show seven to eight neutral electronic bands, most of which are vibrationally resolved. Most of the low-lying electronic states have not been observed previously. We assign the ground states and determine bond lengths and vibrational frequencies for the anions. For the neutral dimers, molecular constants (ω_e , r_e , and T_e) are obtained for most of the low-lying electronic states, and the adiabatic electron affinities are precisely measured. Combining previous experimental results and *ab initio* calculations on Sn_2 and Pb_2 with our data, we make plausible assignments for the electronic terms of each band.

II. EXPERIMENTAL METHODS

The negative ion photoelectron spectrometer^{15,18} and metal cluster anion source^{19,20} have been described in detail previously. Briefly, metal cluster anions are produced in a flowing afterglow ion source by cathodic sputtering with a dc discharge. The cathode is fabricated from high purity tin, lead, or a 1:1 tin-lead alloy to produce the corresponding metal dimer anions. The cathode is cylindrical, 1 cm in diam and 4 cm in length. A mixture of argon (5–10 %) in helium flows over the metal cathode at a flow tube pressure of 0.4 Torr. The cathode is negatively biased at 2–2.5 kV with respect to the grounded flow tube, producing a 5–10 mA discharge. Cluster ions are produced from sputtering of the metal cathode by Ar^+ and other cations, possibly followed by further clustering in the discharge plasma. Since approximately 10–20 W are dissipated at the metal cathode, a water cooling system is necessary to keep the cathode near room temperature and prevent it from melting. Cooling water flows through the metal cathode support via tubing in the electrical feedthrough, and also through tubing surrounding the flow tube. The gas composition, flow rate, and dc voltage are adjusted to optimize the cluster anion yields.

Ion beams of all three species are relatively easy to produce with the cathode discharge ion source. Although optimal ion yields are obtained using the appropriate cathode, one can generate sufficient quantities of all three dimer anions using only the tin-lead alloy cathode. Typical ion currents are 30 pA (Sn_2^- and SnPb^-) and 20 pA (Pb_2^-). Other small bare metal or bimetal clusters, such as trimers and tetramers, can also be produced with this ion source. Unlike the transition metal clusters produced with the same type of ion source, the tin and lead ion sources are insensitive to minor residual oxygen in the system.

After being extracted from the flow tube into a low pressure region, the anions are focused into a beam and mass selected by a Wien filter. The mass selected ion beam is further focused and then sent into the interaction region, where the 40 eV ion beam is crossed by a cw argon ion laser beam with 351.1 nm wavelength (3.531 eV). Photoelectrons ejected into an acceptance cone of 5° half angle are collected perpendicularly to the ion and laser beam plane, and kinetic energies are measured in a hemispherical electrostatic energy analyzer.¹⁵ The transition energies between the anions

and the corresponding neutral species are determined from the difference between the photon energy ($h\nu$) and the measured photoelectron kinetic energy ($e\text{KE}$).

We calibrate the electron kinetic energy scale using the photoelectron spectrum of O^- . The absolute kinetic energy is calibrated against the precisely known oxygen atomic electron affinity.²¹ Spectra are also corrected for an energy scale compression factor,¹⁵ which is calibrated on the known energy level spacings of the tungsten atom.²² The instrumental resolution function of the photoelectron spectrometer is determined by observing the shapes of atomic transitions, and can be approximated by a Gaussian with an 8–10 meV FWHM. The experimental uncertainty of the absolute electron kinetic energy of well-resolved peaks is ± 0.006 eV.

Since the direction of the ejected electron detection is fixed, the angle between the electron detection and the electric field of the laser light can be conveniently changed by rotating a $\lambda/2$ waveplate.²³ The photoelectron angular distribution is then determined by measuring the relative intensities as a function of the laser polarization direction. The angular distribution of the photoelectron intensity obtained with linearly polarized light is given by²⁴

$$d\sigma/d\Omega = (\sigma/4\pi) \cdot [1 + \beta(3 \cos^2 \theta - 1)/2], \quad (1)$$

where θ is the angle between the laser electric field and the direction of electron detection, σ is the total photodetachment cross section, and β is the asymmetry parameter which varies from -1 to 2 . The photoelectron spectra in Fig. 1 are taken at the “magic” angle of $\theta = 54.7^\circ$, which gives intensities proportional to the total photodetachment cross section.

III. RESULTS AND ANALYSIS

A. Photoelectron spectra

The photoelectron spectra of Sn_2^- , SnPb^- , and Pb_2^- are shown in Fig. 1. The photoelectron intensity is plotted as a function of the electron binding energy ($e\text{BE} = h\nu - e\text{KE}$), in the range 1.2–3.4 eV. No transitions are observed below 1.2 eV. The three spectra are very similar, and all exhibit numerous electronic bands which correspond to the low-lying electronic states of the neutral dimers. Seven or eight primary electronic bands are observed; they are labeled a–g or h in Fig. 1. Among those bands, a, b, and f are broad and relatively weak, and c and d (and g in Sn_2^-) are narrow and strong. Given the thermal ion source ($T = 300$ – 400 K), we expect only the lowest anion electronic state to be significantly populated. Accordingly, all of the electronic transitions in the spectra are assigned as originating from the anion electronic ground state. The energy of band a is lowest and is assigned to the ground state of the neutral dimers.

The spectra show vibrational structure for most of the electronic bands of the three dimers. Because the anions are vibrationally excited, the anion vibrational temperatures (T_{vib}) can be estimated from the intensity of the vibrational hot bands. Franck–Condon analyses of the Sn_2^- , Pb_2^- , and SnPb^- spectra indicate a T_{vib} of 350 ± 50 K for Sn_2^- and Pb_2^- , and 450 ± 50 K for SnPb^- . The rotational temperature is usually lower than the vibrational temperature, since rotational relaxation by collisions with the buffer gas in the

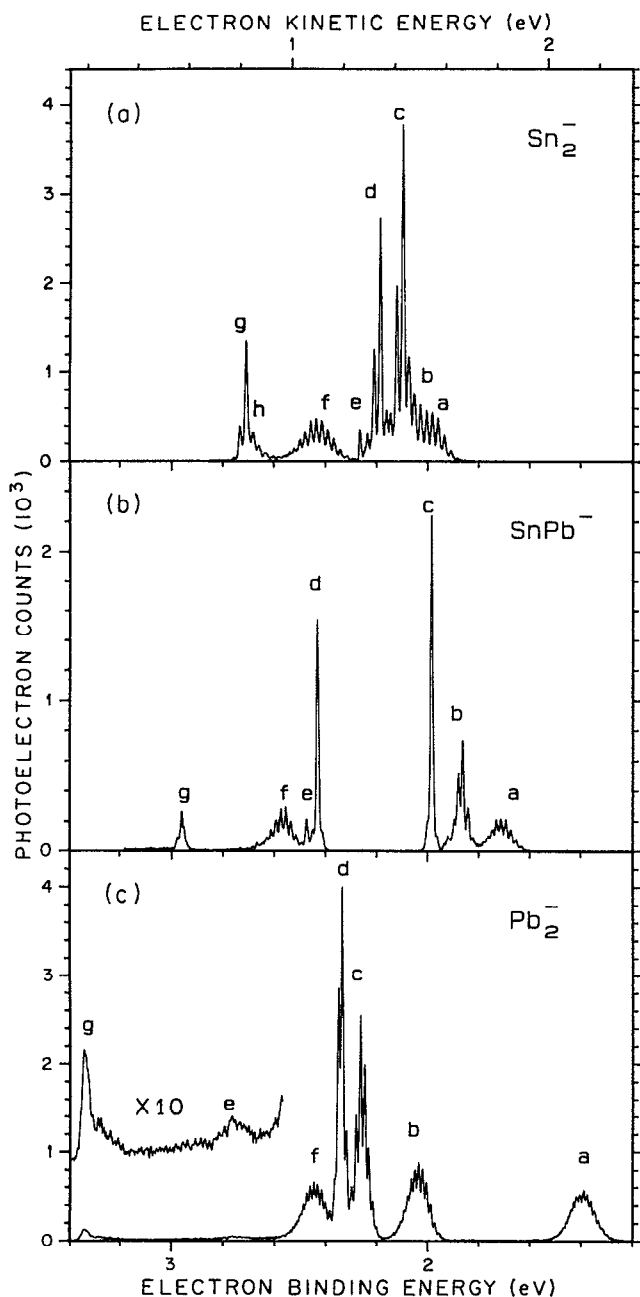


FIG. 1. The photoelectron spectra of Sn_2^- , SnPb^- , and Pb_2^- . All the spectra are displayed over the same electron binding energy range. The electronic bands are labeled in bold letters, but are not shown in alphabetical order to make comparison of the three spectra easier.

flow tube is more efficient than vibrational relaxation.^{18,25} Because of the low rotational temperatures and the small rotational constants for these heavy metal dimers, the contribution of rotational broadening to the line shapes is negligible.

B. Franck-Condon analyses

1. Sn_2^-

The Sn_2^- spectrum in Fig. 1 (a) contains eight electronic transitions. Although bands **a** and **b** are not obviously distin-

guishable, there are several reasons for our assignment of the feature to two bands. First, the Pb_2^- and SnPb^- spectra clearly show two broad bands **a** and **b** in the corresponding regions. Second, band **f** in Sn_2^- and bands **a**, **b**, and **f** in the Pb_2^- spectrum all show normal Franck-Condon profiles. However, after subtracting band **c**, the residual Sn_2^- spectrum exhibits a profile which is either (1) a single badly perturbed progression or (2) two normal overlapping progressions. Third, the assignment of **a** and **b** as two bands is consistent with the theoretical prediction¹² that the two lowest electronic states of Sn_2 are spin-orbit states $^3\Sigma_g^-(0_g^+)$ and $^3\Sigma_g^-(1_g)$, with a splitting of 340 cm^{-1} . All of these observations argue that **a** and **b** represent two different progressions in the Sn_2^- spectrum.

The molecular constants of the electronic transitions were obtained from a Franck-Condon analysis. Franck-Condon factors are computed by numerical integration of the overlap between the anion and neutral Morse oscillator wave functions; the details have been described previously.^{20,23} Bands **d** and **f** were analyzed first because these bands are better separated than bands **a** and **b**. We fit both the Sn_2^- and Sn_2 constants simultaneously, as molecular constants for either state have not been determined. The Franck-Condon simulations of bands **d** and **f** extract the electron binding energies of the transition origins, and the vibrational frequencies of the anion and neutral. The anion vibrational temperature, $350 \pm 50\text{ K}$, is consistent with measurements for other metal dimers produced in the same source.^{19,20} Band **d** exhibits a short vibrational progression; therefore, only the magnitude of the geometry change can be determined by the Franck-Condon analysis. For band **f**, the direction of geometry change can be determined, owing to the observation of a large number of hot bands and a relatively long vibrational progression. The expanded spectrum of band **f** and the optimized fit are shown in Fig. 2. Using the same fitting procedure as for band **d** and anion constants

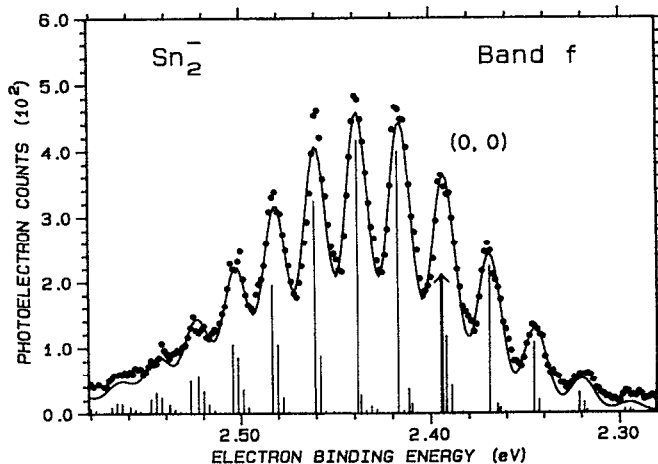


FIG. 2. Franck-Condon fit of band **f** of Sn_2^- . The dots represent the experimental data, and the solid line is the Franck-Condon simulation. The sticks represent single vibrational transitions. An arrow marks the vibrational transition origin ($v' = 0 - v'' = 0$).

obtained above, band c can now be modeled and the neutral molecular constants determined.

The simulations of bands a and b are simplified once the anion constants (ω_e'' , $\omega_e x_e''$, and T_{vib}) have been obtained from the analysis of bands c, d, and f. The simulated c band is first subtracted from the experimental spectrum, and then the residual spectrum is fitted to the sum of the a and b simulation spectra. For band a, molecular constants (r_e , ω_e , and $\omega_e x_e$) of the ground state are well known from high resolution optical spectroscopy.¹ In the simulation, the vibrational origin, the neutral vibrational frequency, and the bond length change are allowed to vary, while the other constants are constrained at previously determined values. Although several origin assignments were attempted, only one choice yielded both a satisfactory fit and vibrational temperature (350 ± 50 K). Shifting the origin one vibrational quantum in either direction resulted in a T_{vib} of 530 or 200 K, respectively, ruling out these origin assignments. The simulation yields the neutral vibrational frequency of $186 \pm 15 \text{ cm}^{-1}$, consistent with the previous optical value of 189.74 cm^{-1} for the Sn_2 ground state.⁴ This simulation determines the electron affinity, $EA(\text{Sn}_2) = 1.962 \pm 0.010$ eV. The determination of the geometry change for band a is less accurate than for the previous bands because of the overlap of bands a and b. In the simulation, varying Δr_e over a range of $\pm 0.006 \text{ \AA}$ does not greatly degrade the quality of the fit, as the change can be partially compensated for by adjusting the intensity of the origin transition.

The band b analysis also presents difficulties, due to the overlap of the bands a and b. In the simulation, different vibrational origins are attempted; the parameters, r_e' and ω_e' , are assumed to be similar to those of band a since they are a pair of spin-orbit states with a small splitting, and are only allowed to vary slightly from the values for band a. The simulation determines the origin position, and yields r_e' and ω_e' . Although we believe that the present assignment is correct, we cannot absolutely exclude other assignments, such as shifting the origin one quantum up or down from the present position. Accordingly, we give an error bar for the term ener-

gy of band b that accounts for several possible origin assignments.

Using the r_e'' obtained from the analysis of band a, we can determine the neutral bond lengths for b, c, d, and f, and analyze band g in the same manner as for bands c and d. Band e contains a single vibrational peak, so only the peak position is given. Band h appears on the right shoulder of band g, and a preliminary Franck-Condon simulation was performed on this band. The results of all of the Franck-Condon analyses are summarized in Table I.

2. Pb_2^- and SnPb^-

The Pb_2^- spectrum in Fig. 1(c) shows seven bands. The first five bands (a-f) are the strongest and are also vibrationally resolved. Band f is labeled ahead of band e for easy comparison among the three spectra. The procedure of the Franck-Condon analysis is nearly the same as for Sn_2 . Starting with bands b and c, the Franck-Condon simulation extracts molecular constants ($\Delta r_e = r_e' - r_e''$, ω_e' , and ω_e''), and determines the electron binding energies of the transition origins and the anion vibrational temperature (350 ± 50 K). Using the anion molecular constants, we then simulate band a. The molecular constants of the Pb_2 ground state are well known from optical spectroscopy.¹ Fixing all the known parameters, the simulation generates r_e'' and $\omega_e x_e''$, and determines the electron affinity, $EA(\text{Pb}_2) = 1.366 \pm 0.010$ eV. Using the anion molecular parameters just obtained, we can analyze bands d and f, and determine the neutral bond lengths of b, c, d, and f. The direction of the geometry change is determined unambiguously for band c, but not for band d. We assume bands c and d have the same direction of geometry change because they involve detachment from the same molecular orbital, as is explained in Sec. IV. The expanded spectrum of bands b and c, and their simulations are displayed in Fig. 3.

There are two weak transitions e and g in the high energy region. The transmission function of the electron analyzer declines rapidly above 3.2 eV binding energy (low electron

TABLE I. The molecular constants of Sn_2 electronic states.

Band	T_0 (eV)	ω_e (cm^{-1})	$\omega_e x_e$ (cm^{-1})	r_e (\AA)	β (± 0.10)	eKE (eV)
Sn_2	-1.962 ± 0.010	200 ± 15	0.7 ± 0.3	2.659 ± 0.012		
Sn_2^{a}	0	186 ± 15	0.49^{a}	2.746^{a}	0.32	1.57
b	$0.094 \pm 0.030^{\text{c}}$	192 ± 20		2.742 ± 0.020	0.27	1.48
c	0.136 ± 0.008	198 ± 15		$(2.659 + 0.044)^{\text{b}} \pm 0.020$ or $(2.659 - 0.038) \pm 0.020$	0.55	1.43
d	0.225 ± 0.008	199 ± 15		$(2.659 + 0.043)^{\text{b}} \pm 0.020$ or $(2.659 - 0.037) \pm 0.020$	0.64	1.34
e	0.304 ± 0.010				0.20	1.26
f	0.432 ± 0.010	181 ± 15	0.5 ± 0.3	2.772 ± 0.018	-0.17	1.14
g	0.751 ± 0.012	194 ± 15		$(2.659 + 0.031)^{\text{b}} \pm 0.020$ Cor $(2.659 - 0.031) \pm 0.020$	0.87	0.82
h	$0.70 \pm 0.03^{\text{c}}$	185 ± 25			-0.50	0.87

^aThe molecular parameters are from Ref. 4, and they are fixed in the Franck-Condon simulation.

^bThe sign of the bond length changes cannot be determined by the Franck-Condon analysis.

^cWe give larger error bars because the transition origin is not certainly assigned, see text.

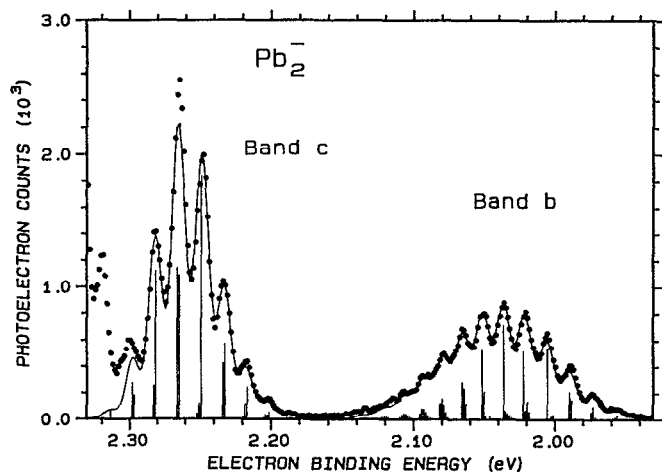


FIG. 3. Franck-Condon fits of bands b and c of Pb_2^- . The dots represent the experimental data, and the solid line is the Franck-Condon simulation. The sticks represent single vibrational transitions.

kinetic energies), and both the sensitivity and resolution decrease. The intensity and band shape of band g are likely to be affected by this decline. The right shoulder of band g might be attributable to an additional electronic state. Except for the measurement of the band positions, no detailed analyses were attempted for bands e and g. The results of the analysis are summarized in Table II.

The SnPb^- spectrum in Fig. 1(b) is similar to its homonuclear congeners. However, the separation of bands c and d is substantially greater. The procedure of the Franck-Condon simulation is nearly the same as above. We analyze band b first to extract the anion vibrational frequency and temperature which is determined to be 450 ± 50 K. Again, we cannot determine the direction of the bond length changes for the sharp bands, c, d, and g, from the Franck-Condon analysis. The electron affinity is determined to be $EA(\text{SnPb}) = 1.699 \pm 0.008$ eV. The other constants are listed in Table III.

C. Angular distribution measurements

The measurements of the angular distributions were performed by taking the full spectra at $\theta = 0^\circ$ and $\theta = 90^\circ$,

and normalizing to the integration time, ion current, and laser power. To determine β accurately for a single peak, the angular dependence of the largest peak in each spectrum was carefully measured in 10° increments, and the observed intensities were fit to Eq. (1). This accurately determined β was then used to properly scale the $\theta = 0^\circ$ and $\theta = 90^\circ$ spectra with respect to one another.

The results of the angular distribution measurements, given in Tables I–III, show that the broad bands (a, b, and f) and the sharp bands (c, d, and g) have different angular dependencies on eKE . Specifically, β decreases from positive to negative as one proceeds through the broad bands, a, b, and f, while β is always positive and increases as one proceeds through the sharp bands, c, d, and g. This difference can be attributed to the removal of an electron from different molecular orbitals. Band e in Sn_2^- or SnPb^- shows a single vibrational peak and an angular dependence which does not fit into either category. The shape and β of band h in Sn_2^- behaves like the other broad bands. The angular distributions provide insight into the nature of the photodetachment processes, and aid in assigning the individual electronic bands, as we will discuss in Sec. IV.

D. Thermochemistry

The electron affinities of Sn and Pb atoms^{21,26} have been determined by photoelectron spectroscopy. The relation $D_0(M_2^-) - D_0(M_2) = EA(M_2) - EA(M)$ can be employed to determine the dissociation energy difference between the anion and neutral dimers, where M represents Sn or Pb. The values of $D_0(\text{Sn}_2^-) - D_0(\text{Sn}_2) = 0.850 \pm 0.014$ eV and $D_0(\text{Pb}_2^-) - D_0(\text{Pb}_2) = 1.002 \pm 0.018$ eV are therefore precisely measured by photoelectron spectroscopy. In addition, using the already known values of $D_0(\text{Sn}_2) = 1.901 \pm 0.003$ eV (Ref. 7) and $D_0(\text{Pb}_2) = 0.86 \pm 0.01$ eV,¹¹ the values of $D_0(\text{Sn}_2^-) = 2.751 \pm 0.017$ eV and $D_0(\text{Pb}_2^-) = 1.86 \pm 0.03$ eV are derived. Both anion dissociation energies are substantially larger than the corresponding neutral dissociation energies. The lowest dissociation asymptote of SnPb^- is $\text{Sn}^-(5p^3, ^4S_{3/2}) + \text{Pb}(6p^2, ^3P_0)$, and the alternative dissociation asymptote $\text{Sn}(5p^2, ^3P_0) + \text{Pb}^-(6p^3, ^4S_{3/2})$ is 0.8 eV higher. The dissociation energy difference $D_0(\text{Sn}^- - \text{Pb}) - D_0(\text{SnPb}) = EA(\text{SnPb}) - EA(\text{Sn})$ is

TABLE II. The molecular constants of Pb_2^- electronic states.

Band	T_0 (eV)	ω_e (cm^{-1})	$\omega_e x_e$ (cm^{-1})	r_e (\AA)	β (± 0.10)	eKE (eV)
Pb_2^-	-1.366 ± 0.010	129 ± 15	0.2 ± 0.2	2.814 ± 0.008		
Pb_2 a	0	110 ± 15	0.316^a	2.9271^a	0.48	2.17
b	0.657 ± 0.010	120 ± 15	0.2 ± 0.2	2.902 ± 0.014	0.15	1.51
c	0.883 ± 0.010	132 ± 15	0.4 ± 0.3	2.759 ± 0.014	0.28	1.28
d	0.972 ± 0.010	124 ± 20		2.779 ± 0.014	0.38	1.19
f	1.054 ± 0.012	118 ± 15	0.3 ± 0.2	2.919 ± 0.014	-0.30	1.12
e	~1.4					0.76
g	~1.9					0.2

^aThe molecular constants are from Ref. 6, and are fixed in the Franck-Condon analysis.

TABLE III. The molecular constants of SnPb electronic states.

Band	T_0 (eV)	ω_e (cm^{-1})	$\omega_e x_e$ (cm^{-1})	r_e (Å)	β (± 0.10)	eKE (eV)
SnPb^-	-1.699 ± 0.008	161 ± 15		r_e^a		
SnPb a	0	148 ± 15	0.4 ± 0.3	$(r_e' + 0.085) \pm 0.008$	0.39	1.83
b	0.169 ± 0.008	148 ± 15	0.3 ± 0.2	$(r_e' + 0.045) \pm 0.008$	0.28	1.66
c	0.291 ± 0.008	145 ± 20		$r_e' \pm 0.025^b$	0.32	1.54
d	0.737 ± 0.008	158 ± 20		$r_e' \pm 0.025^b$	0.42	1.10
e	0.780 ± 0.010				-0.44	1.05
f	0.861 ± 0.010	158 ± 15	0.8 ± 0.3	$(r_e' + 0.075) \pm 0.008$	-0.10	0.97
g	1.268 ± 0.012	153 ± 25		$r_e' \pm 0.035^b$	0.62	0.57

^aThe bond length r_e' of the anion ground state, which cannot be determined from this work.

^bThe sign of the bond length changes cannot be determined by the Franck-Condon analysis; therefore, the magnitude of the bond length change is included in the error bar.

accurately determined to be 0.587 ± 0.012 eV, which again demonstrates that the bond in the anion is stronger than in the neutral. There is no experimental measurement of D_0 (SnPb) presently available.

IV. DISCUSSION

A. General observations

The heavy group IV dimers share several common characteristics. The three spectra are remarkably similar, all exhibiting a small number of discernible low-lying electronic bands. This reflects the simple valence electron configuration of the constituent atoms. Each atom has a $5s^2 5p^2$ or $6s^2 6p^2$ configuration, and contributes two p valence electrons for bonding. The interactions among these p electrons are expected to dominate the bonding and electronic structure in the dimers. Except for the large difference in relativistic effects,²⁷ the basic interactions of the p atomic orbitals are similar for tin and lead. For heavy-atom molecules, such as Sn_2 and Pb_2 , a simple spin (S)–orbital angular momentum (Λ) coupling scheme is not a good description of electronic states, since the good electronic quantum number is $\Omega = \Lambda + S$. Because the Λ - S coupling scheme provides a good intuitive picture for the dominant electronic configurations, we still use the Λ - S labeling or the combined labeling scheme $^{2S+1}\Lambda(\Omega)$ [e.g., $^3\Pi_u(1_u)$]. After removal of the g and u subscripts, we obtain the states corresponding to SnPb , such as $^3\Pi(1)$.

The ground states of Sn_2 and Pb_2 , well characterized by high resolution optical spectroscopy,¹ are $^3\Sigma_g^-(0_g^+)$ with the valence molecular orbital configuration $1\sigma_g^2 1\sigma_u^2 1\pi_u^2 2\sigma_g^2$ (or $1\pi_u^2 2\sigma_g^2$). These states correlate to the lowest dissociation asymptote: $^3P_0 + ^3P_0$. By analogy, the SnPb ground state is tentatively assigned to $X^3\Sigma^-(0^+)$ with the configuration, $1\pi^2 3\sigma^2$. The two likely MO configurations for the anion ground state are $1\pi_u^3 2\sigma_g^2$ or $1\pi_u^4 2\sigma_g^1$ for Sn_2^- and Pb_2^- ($1\pi^3 3\sigma^2$ or $1\pi^4 3\sigma^1$ for SnPb^-). We indicated earlier that band **a** arises from the anion to neutral ground state transition for Sn_2 and Pb_2 . If we assume further that the photodetachment transition involves only a simple one-electron process, then $1\pi_u^3 2\sigma_g^2$ is the most likely configura-

tion of the anion ground state. This last assumption is likely valid for a strong transition, such as that giving rise to band **a**, because single electron processes (i.e., detachment with no additional electron reorganization) give rise to the strongest photoelectron transitions.²⁸ The configuration $2\sigma_g^2 1\pi_u^3$ can only form a $^2\Pi_u$ state, and the spin-orbit interaction splits it into two components: $^2\Pi_u(1/2)$ and $^2\Pi_u(3/2)$. The $^2\Pi_u(3/2)$ state is the favored ground state in terms of Hund's rule. Therefore, we assign the ground state $^2\Pi_u(3/2)$ to Sn_2^- and Pb_2^- , and $^2\Pi(3/2)$ to SnPb^- .

All of the observed strong transitions should arise from detachment of an electron from either the $1\pi_u$ or $2\sigma_g$ orbital. Detaching a π_u electron produces $^3\Sigma_g^-(0_g^+, 1_g)$, $^1\Delta_g(2_g)$, and $^1\Sigma_g^+(0_g^+)$ states; detaching a σ_g electron generates $^3\Pi_u(0_u^+, 0_u^-, 1_u, 2_u)$ and $^1\Pi_u(1_u)$ states. The possible electronic states are listed in Table IV.

B. Photoelectron angular distributions

The angular distribution measurements provide additional information about the molecular orbitals. The asymmetry parameter β for photoelectron emission is a function of both the symmetry of the orbital from which the electron is detached and the electron kinetic energy.²⁴ Early negative ion photoelectron studies showed^{29,30} that β is 2 and independent of eKE for s -electron detachment from H^- and atomic alkali metal anions. For photoelectrons ejected from a p orbital, the angular distribution at threshold is nearly

TABLE IV. The possible MO configurations and the related terms in both Λ - S and ω - ω coupling.

	MO config.	Λ - S coupling	ω - ω coupling
Sn_2	$\sigma_g^2 \pi_u^2$	$^3\Sigma_g^-; ^1\Delta_g; ^1\Sigma_g^+$	$0_g^+, 1_g; 2_g; 0_g^+$
	$\sigma_g^1 \pi_u^3$	$^3\Pi_u; ^1\Pi_u$	$0_u^+, 0_u^-, 1_u, 2_u; 1_u$
	π_u^4	$^1\Sigma_g^+$	0_g^+
Sn_2^-	$\sigma_g^2 \pi_u^3$	$^2\Pi_u$	$(3/2)_u, (1/2)_u$

isotropic. As the electron kinetic energy increases to around 1 eV above threshold, β decreases to ≈ -1 (a $\sin^2 \theta$ distribution). From this point it increases toward $\beta \approx 2$ (a $\cos^2 \theta$ distribution) as $e\text{KE}$ increases. The dependence of the asymmetry parameters for p -electron detachment on $e\text{KE}$ has been verified in several investigations, including recent studies on O^- by Hanstorp *et al.*³¹ and halogen atomic anions by Radojević *et al.*,³² and measurements in this laboratory of the halogen atomic anions³³ and Bi^- .³⁴

For diatomics, the $e\text{KE}$ dependence of β is significantly more complex than that for atoms. Only a qualitative explanation is given in this work. The photoelectron spectra of the metal dimers involve electronic transitions with either $p\sigma_g$ or $p\pi_u$ electron detachment, and the angular distributions are expected to be different for these two processes. Our measurements show that the observed energy dependence of β for the relatively broad bands (a, b, and f) is very similar to atomic p -electron detachment. This implies that these electronic bands arise from p -like detachment. We have also found that the asymmetry parameters in the photoelectron spectra of Bi^- (p detachment) and Bi_2^- ($p\pi$ detachment) show similar $e\text{KE}$ -dependent behavior.³⁴ Given that band a is already assigned to the ground state transition with a $p\pi$ electron detachment, we can tentatively conclude that bands a, b, and f arise from $p\pi$ electron detachment, and can be assigned to states with a $\sigma_g^2\pi_u^2$ configuration (see Table IV). The pattern for bands c, d, and g is different from the former one (more s -like), suggesting that these bands arise from $p\sigma_g$ electron detachment, and can be assigned to states with $\sigma_g^1\pi_u^3$ configuration. The difference in the angular distributions between the $p\sigma_g$ and $p\pi_u$ electron emissions can be explained qualitatively. Mixing of the $p\sigma_g$ and $s\sigma_g$ orbitals is expected to be important for heavy systems,³⁵ and this effect could contribute to the partial s character of the $p\sigma_g$ orbital. The data demonstrate that the measurement of angular distributions is a sensitive method of probing the molecular orbitals of metal dimers.

The results of the angular distribution measurements combined with the Franck-Condon analyses show that small geometry changes result from the $2\sigma_g$ electron detachment and large geometry changes arise from $1\pi_u$ electron detachment. We thus conclude that $2\sigma_g$ (or 3σ) is a weakly bonding or nonbonding orbital, and $1\pi_u$ is a strongly bonding orbital. According to simple MO arguments, $2\sigma_g$ is expected to be a bonding orbital formed from the p_z orbitals along the internuclear axis; $1\pi_u$ is another bonding orbital formed from the p_x and p_y orbitals of the two atoms. A Mulliken population analysis by Andzelm *et al.*¹⁴ predicts that the $2\sigma_g$ (3σ in heteronuclear diatomics) orbitals in the group IV diatomics (Si_2 , Ge_2 , Sn_2 , SiGe , SiSn , GeSn) are essentially nonbonding, but the authors gave no further explanation. Mixing of the $p\sigma_g$ orbital with the $s\sigma_g$ orbital, for which the angular distributions provide evidence, could considerably reduce the electron density between the two nuclei, consequently reducing the bonding character of the $p\sigma_g$ orbital.³⁵ Our data show that the dissociation energies increase considerably upon adding an electron to the π_u orbital. Therefore, the $p\pi$ orbitals appear to dominate the metal bonding for the tin and lead dimers. In the case of Pb_2 , the

anion dissociation energy is almost twice as large as for the neutral dimer; however, the bond order only increases from 1 to 1.5, assuming that $p\sigma_g$ is a nonbonding orbital. *Ab initio* calculations show¹ that the anomalously small dissociation energy of Pb_2 is the result of spin-orbit interactions, a relativistic effect.

Recently, Wang *et al.*³⁶ have reported the photoelectron spectra of heavy group IV-VI neutral diatomics. The ground state of the cations (SnSe^+ , SnTe^+ , PbTe^+ , and PbTe^+) was deduced to be $^2\Pi_{3/2}$; we find the same ground state for the isoelectronic group IV dimer anions. In addition, Wang *et al.*³⁶ found that the spectra for all four diatomic species exhibited both broad and very narrow electronic band structure. They provided an explanation of the spectra that is similar to ours: the sharp, strong bands arise from removal of electrons from the nonbonding or weakly bonding 3σ orbital, and the broad bands arise from removal from the strongly bonding π orbital. While the situations are similar for both experiments, the angular distribution measurements in this work provide additional experimental evidence to support the conclusions of Wang *et al.*

C. Sn_2 and Pb_2 assignments

Since none of the electronically excited states in the photoelectron spectra has been previously observed, *ab initio* calculations are extremely important to the assignments. With the aid of Balasubramanian and Pitzer's¹² calculations of the molecular constants of the low-lying electronic states, we can assign most of the bands in the Sn_2^- and Pb_2^- spectra. For Sn_2 , the assignments are listed in Table V. Band a is assigned to the ground state $X^3\Sigma_g^-(0_g^+)$. The band shapes and angular distribution measurements suggest that bands a, b, and f have the same g symmetry (π_u detachments), and bands c, d, and g have the same u symmetry (σ_g detachments). Except for band b, the energy levels of most of the excited states are systematically overestimated by the calculations. Band b is labeled as A, consistent with the identically labeled band of Pb_2 . The term energy for A $^3\Sigma_g^-(1_g)$ is not accurately determined in this work because of the uncertain origin assignment. Bands c and d are assigned to the $^3\Pi_u(2_u)$ and $^3\Pi_u(1_u)$ states. Based on the similarities of bands c and d in the Sn_2^- and Pb_2^- spectra, the bond lengths of the neutral states (c and d) for Sn_2 are assumed to be smaller than that of the anion ground state, as is true for Pb_2 . Band f is assigned to $^1\Delta_g(2_g)$. A state lying $3000\text{--}5000\text{ cm}^{-1}$ above the ground state was detected in optical emission spectra.⁸ The most favorable candidate is 2_g because it is the only state lying (3495 cm^{-1}) within the predicted energy range.

The assignments of the remaining three bands are less certain. Band e shows only a single vibrational peak, unlike either the broad or the sharp bands. Comparison with *ab initio* calculations suggests an assignment of either $^3\Pi_u(0_u^-)$ or $^3\Pi_u(0_u^+)$. However, this assignment is not consistent with the angular distribution measurement because β for band e is considerably smaller than the β 's for the other sharp bands (c, d, and g). Another possible assignment for band e is $^1\Sigma_g^+(0_g^+)$ with a π_u^4 configuration; the transition

TABLE V. Spectroscopic parameters of Sn_2 electronic states.^a

Band	S State	Constant	This work	Previous value	<i>Ab initio</i> ^b
a	$X^3\Sigma_g^-(0_g^+)$	T_e	0	0	0
		ω_e	186 ± 15	189.74^c	197
		r_e		2.746^c	2.76
b	$A^3\Sigma_g^-(1_g)$	T_e	760 ± 250		342
		ω_e	192 ± 20		205
		r_e	2.742 ± 0.020		2.75
c	$^3\Pi_u(2_u)$	T_e	1095 ± 65		1447
		ω_e	198 ± 15		218
		r_e	2.621 ± 0.020^d		2.62
d	$^3\Pi_u(1_u)$	T_e	1815 ± 65		2509
		ω_e	199 ± 15		220
		r_e	2.622 ± 0.020^d		2.62
e	?	T_e	2450 ± 80		
f	$B^1\Delta_g(2_g)$	T_e	3495 ± 80	$3000\text{-}5000^e$	7159
		ω_e	181 ± 15	195^e	178
		r_e	2.772 ± 0.018		2.81
g	$^1\Pi_u(1_u)?$	T_e	6060 ± 100		7260
		ω_e	194 ± 15		232
		r_e	2.628 ± 0.020		2.62
h	$^1\Sigma_g^+(0_g^+)?$	T_e	5650 ± 250		8002
		ω_e	185 ± 25		116
		r_e			2.78

^aAll units are in cm^{-1} , except for r_e (\AA).

^bSee Refs. 1 and 12.

^cThe data are from Ref. 4.

^d r_e value is determined by assuming the minus sign for the corresponding r_e in Table I.

^eThe data are from Ref. 8.

would then arise from a two-electron process in which a σ_g electron is detached and another σ_g electron is promoted to the π_u orbital. The weak integrated intensity of band e might imply that it results from a two-electron process. Thus, no assignment is attempted for band e. Band g is tentatively assigned to $^1\Pi_u(1_u)$ based on *ab initio* calculations, and the geometry change for this band is assumed in the same manner as for bands c and d. A likely assignment for band h is $^1\Sigma_g^+(0_g^+)$; weak intensity and overlap with band g render determination of the transition origin for band h difficult. The molecular constants from previous experiments and *ab initio* calculations are also summarized in Table V.

The assignments for the Pb_2^- spectrum are shown in Table VI. As for Sn_2 , the ground state $X(0_g^+)$ is assigned to band a. The assignments of the first four excited bands b, c, d, and f are in excellent agreement with the calculations.¹² In previous emission spectra,^{3,8} a low-lying state $\leq 5500 \text{ cm}^{-1}$ above the ground state was found, which Bondybey and English labeled state A. Later, Balasubramanian and Pitzer suggested¹² that the most probable assignment for this A state is 1_g ; however, they could not eliminate the assignment of $A(2_u)$. We assign band b to 1_g , and find that the molecular constants (T_e and ω_e) for band b indicate that it is the one observed in the previous experiment.³ Our results confirm Balasubramanian and Pitzer's tentative assignment of

$A(1_g)$, because our measured $T_0(2_u) = 7120 \text{ cm}^{-1}$ is too large for the alternative choice of $A(2_u)$. Based on the assignment of bands a and b, the spin-orbit splitting between the $^3\Sigma_g^-$ components, 0_g^+ and 1_g , is precisely measured at $5300 \pm 80 \text{ cm}^{-1}$. Band f is assigned to $^1\Delta_g(2_g)$.

The assignments of bands e and g are less certain, owing to the weak intensities and the lack of vibrational information. From previous spectroscopic studies³ and *ab initio* calculations,¹ we tentatively assign bands e and g to $B(0_u^-)$ and $C(0_u^+)$, respectively. An alternative assignment of $^1\Sigma_g^+(0_g^+)$ to band e, however, cannot be ruled out. The intensity of band g is stronger than band e even though the sensitivity could be cut off in this region. The right shoulder of band g may be attributed to the overlap of the $C(0_u^+)$ state with a $^1\Sigma_g^+(0_g^+)$ state, which is predicted to lie 490 cm^{-1} below $C(0_u^+)$.¹² Early experiments also detected^{3,8} the $F(0_u^+)$ state, and two other unidentified states, D and E. The term energies of the D, E, and F states are $T_e(A) + 13\,433$, $T_e(A) + 14\,500$, and $19\,855 \text{ cm}^{-1}$, respectively. If the energies of states D and E are calculated using our results for $T_e(A)$, then the energy of E ($19\,800 \text{ cm}^{-1}$) is nearly the same as F. It is likely that states E and F actually correspond to the same state, 0_u^+ . Our assignments, along with previous experimental results and *ab initio* predictions are listed in Table VI.

TABLE VI. Spectroscopic parameters for Pb_2^- electronic states.^a

Band	State	Constant	This work	Previous value	<i>Ab initio</i> ^b
a	$X^3\Sigma_g^-(0_g^+)$	T_e	0	0	0
		ω_e	110 ± 15	110.09^c	103
		r_e		2.9271^c	2.97
b	$A^3\Sigma_g^-(1_g)$	T_e	5300 ± 80	$<5500^d$	4150
		ω_e	120 ± 15	122^d	124
		r_e	2.902 ± 0.014		2.94
c	$^3\Pi_u(2_u)$	T_e	7120 ± 80		6670
		ω_e	132 ± 15		119
		r_e	2.759 ± 0.014		2.70
d	$^3\Pi_u(1_u)$	T_e	7840 ± 80		7570
		ω_e	124 ± 20		119
		r_e	2.779 ± 0.014		2.71
f	$^1\Delta_g(2_g)$	T_e	8505 ± 100		10130
		ω_e	118 ± 15		105
		r_e	2.919 ± 0.014		2.75
e	$B^3\Pi_u(0_u^-)?$ [or $^1\Sigma_g^+(0_g^+)$]	T_e	~ 11300	12457^d	12920
		ω_e			106
		r_e			2.75
g	$C^1\Pi_u(0_u^+)?$	T_e	~ 15300	15311^c	14130
		ω_e		128.15^c	115
		r_e		2.7666^c	2.74

^a All units are in cm^{-1} , except for r_e (\AA).

^b See Refs. 1 and 12.

^c The molecular constants are from Ref. 6.

^d The molecular constants are from Ref. 3.

D. SnPb assignments

Since neither *ab initio* calculations nor spectroscopic data have been reported, the state assignments for SnPb^- are more difficult. However, the SnPb^- spectrum is similar to those of Sn_2^- and Pb_2^- , and preliminary assignments can rely upon comparison of the three spectra. Furthermore, we can extract extra information by correlating the low-lying electronic states with the possible dissociation asymptotes. The lowest asymptote $^3P_0(\text{Sn}) + ^3P_0(\text{Pb})$ should correlate to the ground state. The following two lowest asymptotes are $^3P_1(\text{Sn}) + ^3P_0(\text{Pb})$ and $^3P_2(\text{Sn}) + ^3P_0(\text{Pb})$, with energies of 1692 and 3427 cm^{-1} . For the next asymptotes, the Pb atom is in a spin-orbit excited state and the energies are

much higher than for the first three asymptotes. Since the observed electronic bands in the SnPb^- spectrum are comparable in spacing to those in the Sn_2^- and Pb_2^- spectra, we assume that most of the low-lying electronic states observed in our spectrum correlate to the first three asymptotes (in which the Pb atom is in the ground state).

The assignments of SnPb^- are given in Table VII. Band **a** is assigned to the ground state, $X^3\Sigma^-(0^+)$. Unlike the Sn_2^- or Pb_2^- spectrum, band **b** exhibits an unusual appearance, resembling neither bands **a** and **f** nor bands **c** and **d**. The magnitude of the bond length of the $^3\Sigma^-(1)$ state (band **b**) lies in between the bond lengths of the broad bands (**a** and **f**) and the sharp bands (**c** and **d**) (see Table III). We still assign band **b** to the $^3\Sigma^-(1)$ state with $3\sigma^2 1\pi^2$, but we suggest that

TABLE VII. Electronic states of SnPb^- .

Band	T_0 (cm^{-1}) ^a	State	MO config.	Dissociated atoms
a	0	$X^3\Sigma^-(0^+)$	$3\sigma^2 1\pi^2$	$^3P_0^{\text{Sn}} + ^3P_0^{\text{Pb}}$
b	1363 ± 65	$^3\Sigma^-(1)$	$3\sigma^2 1\pi^2$	$^3P_1^{\text{Sn}} + ^3P_0^{\text{Pb}}$
c	2347 ± 65	$^3\Pi(2)$	$3\sigma^1 1\pi^3$	$^3P_2^{\text{Sn}} + ^3P_0^{\text{Pb}}$
d	5944 ± 65	$^3\Pi(1)$	$3\sigma^1 1\pi^3$	$^3P_2^{\text{Sn}} + ^3P_0^{\text{Pb}}$
e	6291 ± 80	$^3\Pi(0^-)?$	$3\sigma^1 1\pi^3$	$^3P_1^{\text{Sn}} + ^3P_0^{\text{Pb}}$
f	6944 ± 80	$^1\Sigma^+(0^+)$	$3\sigma^2 1\pi^2$	$^3P_2^{\text{Sn}} + ^3P_0^{\text{Pb}}$
g	10226 ± 100	$^3\Pi$ or $^1\Pi?$	$3\sigma^1 1\pi^3$	

^a The observed values in this work.

TABLE VIII. Dissociation asymptotes of some homonuclear (Sn_2 and Pb_2) and heteronuclear (SnPb) molecular states and their energies.

Sn ₂ or Pb ₂			SnPb		
Asymptote	State	Energy ^a	Asymptote (Sn + Pb)	State	Energy ^a (cm ⁻¹)
³ P ₀ + ³ P ₀	0 _g ⁺	0.0	³ P ₀ + ³ P ₀	0 ⁺	0.0
³ P ₁ + ³ P ₀	0 _g ⁻ , 1 _g , 0 _u ⁻ , 1 _u	1 691.8 (Sn ₂)	³ P ₁ + ³ P ₀	0 ⁻ , 1	1 691.8
		or 7 819.4 (Pb ₂)	³ P ₀ + ³ P ₁	0 ⁻ , 1	7 819.4
³ P ₂ + ³ P ₀	0 _g ⁺ , 1 _g , 2 _g , 0 _u ⁺ , 1 _u , 2 _u	3 427.7 (Sn ₂)	³ P ₂ + ³ P ₀	0 ⁺ , 1, 2	3 427.7
		or 10 650.5 (Pb ₂)	³ P ₀ + ³ P ₂	0 ⁺ , 1, 2	10 650.5

^a Atomic energy level, see Ref. 22.

the $3\sigma^2 1\pi^2$ configuration significantly mixes with $3\sigma^1 1\pi^3$ through a spin-orbit interaction between $^3\Sigma^-(1)$ and $^3\Pi(1)$. This interaction vanishes in the homonuclear diatomics because of the different g and u symmetries.

Bands **c** and **d** are assigned to states $^3\Pi(2)$ and $^3\Pi(1)$ with a $3\sigma^1 1\pi^3$ configuration. As in the Sn_2 and Pb_2 spectra, bands **c** and **d** are very sharp and strong; however, the separation between the two bands is much greater in this case. The spin-orbit interaction can also be employed to rationalize this larger splitting. For Sn_2 and Pb_2 , two states, $^3\Sigma_g^-(1_g)$ (band **b**) and $^3\Pi_u(1_u)$ (band **d**), lie relatively close to one another and no interaction occurs between them. For SnPb , the perturbation of the spin-orbit could cause repulsion between the two $\Omega = 1$ states (**b** and **d**). Consequently, the shift of band **d** results in the large separation of bands **c** and **d**.

The large splitting also reflects the available dissociation asymptotes for the heteronuclear diatomics. For Sn_2 and Pb_2 , the dissociation asymptote $^3P_0 + ^3P_1$ correlates to four electronic states: $0_g^-, 0_u^-, 1_g, 1_u$. Both bands **b** and **d** are correlated to this asymptote and are assigned to the $^3\Sigma_g^-(1_g)$ and $^3\Pi_u(1_u)$ states. In SnPb , $^3P_0 + ^3P_1$ correlates to two dissociation asymptotes $^3P_0(\text{Sn}) + ^3P_1(\text{Pb})$ and $^3P_1(\text{Sn}) + ^3P_0(\text{Pb})$, and each asymptote correlates to two electronic states 0^- and 1 (see Table VIII). Since the 1 state correlated to $^3P_1(\text{Sn}) + ^3P_0(\text{Pb})$ is occupied by the lower state, $^3\Sigma^-(1)$ (**b** band), the $^3\Pi(1)$ state (**d** band) must arise from a higher dissociation asymptote. We assume that $^3\Pi(1)$ (**d** band) correlates to the next lowest asymptote $^3P_2(\text{Sn}) + ^3P_0(\text{Pb})$. The 2_u or $^3\Pi(2)$ states (**c** bands) in all three spectra correlate to $^3P_2 + ^3P_0$ or $^3P_2(\text{Sn}) + ^3P_0(\text{Pb})$. Therefore, a qualitative estimate can be made that the band **c** and **d** separation for SnPb should be at least 1735 cm^{-1} (the energy difference between the 2nd and 3rd lowest asymptotes) larger than the separations in Sn_2 and Pb_2 . The measured separation between bands **c** and **d** for SnPb is 3597 cm^{-1} ; in comparison, the corresponding separations in Sn_2 and Pb_2 are 720 cm^{-1} . Table VIII provides a useful reference for following this discussion.

Band **f** should have a $3\sigma^2 1\pi^2$ configuration, as in band **a**. Unlike the band **f** assignments of $^1\Delta_g(2_g)$ for Sn_2 and Pb_2 , the $^1\Sigma^+(0^+)$ state is the only possible assignment for band **f**, since all the other states correlated to the lowest three asymptotes are filled by the lower energy bands. The appearance of band **e** is similar to the identically labeled band for Sn_2 . The obvious assignment for band **e** is $^3\Pi(0^-)$; however, the measured β is negative, implying $p\pi$ detachment, and incompatible with the above assignment. Thus, a definitive assignment is not attempted for this band. Band **g** is quite separated from band **f**, and the angular distribution suggests that band **g** arises from $p\sigma$ detachment. The possible states are $^3\Pi$ or $^1\Pi(0^+ \text{ or } 1)$, which must correlate to a higher dissociation asymptote (where the Pb atom is in an excited state). Our assignments along with the corresponding dissociation asymptotes are given in Table VII.

Comparing the three spectra, we can observe that the spin-orbit splittings between bands **a** and **b** are in the order: $\text{Sn}_2 < \text{SnPb} < \text{Pb}_2$. As expected, the spin-orbit effect increases with the masses of the constituent atoms.²⁷ SnPb has an intermediate spin-orbit splitting, suggesting that the Sn and Pb atomic orbital contributions to the $p\pi$ bonding orbital, where the unpaired electron resides, are of similar magnitude.

V. CONCLUSION

The ultraviolet photoelectron spectra of Sn_2^- , Pb_2^- , and SnPb^- have been observed. The spectra show multiple electronic bands which provide abundant information about the low-lying electronic structures of the three neutral dimers. Franck-Condon analyses yield spectroscopic parameters for the anion ground states and the neutral excited states. The adiabatic electron affinities are determined to be $EA(\text{Sn}_2) = 1.962 \pm 0.010 \text{ eV}$, $EA(\text{Pb}_2) = 1.366 \pm 0.010 \text{ eV}$, and $EA(\text{SnPb}) = 1.569 \pm 0.008 \text{ eV}$. The anion dissociation energies are $D_0(\text{Sn}_2^-) = 2.751 \pm 0.017 \text{ eV}$ and $D_0(\text{Pb}_2^-) = 1.86 \pm 0.03 \text{ eV}$, both of which are significantly larger than those of the neutral dimers. The angular distribution measurements show that the electron kinetic energy de-

pendence of the angular distributions is different for $p\sigma$ and $p\pi$ electron detachment. This measurement, along with the Franck–Condon profiles, provides information about the molecular orbital from which the photoelectron is ejected. Using previous experimental results, *ab initio* calculations, and the present data, we have assigned most of the observed electronic bands to low-lying electronic states of the neutral species. The present experiment provides an overview of the low-lying electronic states of the group IV heavy metal dimers. In addition, the photoelectron spectrum of SnPb^- provides the first spectroscopic investigation of SnPb^- , and offers spectroscopic data which we hope will inspire new theoretical studies.

ACKNOWLEDGMENTS

We are grateful to Dr. Gustav Gerber for extensive discussions concerning main group metal clusters, which stimulated this study. We also thank Hans Rohner from the JILA mechanical shop for his help with the fabrication of the metal cathodes. This research was supported by National Science Foundation Grants No. CHE88-19444 and No. PHY90-12244.

- ¹ K. Balasubramanian, *Chem. Rev.* **90**, 93 (1990).
- ² V. E. Bondybey and J. H. English, *J. Mol. Spectrosc.* **84**, 388 (1980).
- ³ V. E. Bondybey and J. H. English, *J. Chem. Phys.* **67**, 3405 (1977).
- ⁴ V. E. Bondybey, M. C. Heaven, and T. A. Miller, *J. Chem. Phys.* **78**, 3593 (1983).
- ⁵ V. E. Bondybey and J. H. English, *J. Chem. Phys.* **76**, 2165 (1982).
- ⁶ V. E. Bondybey and J. H. English, *J. Chem. Phys.* **74**, 6978 (1981); M. C. Heaven, T. A. Miller, and V. E. Bondybey, *J. Phys. Chem.* **87**, 2072 (1983).
- ⁷ K. Pak, M. F. Cai, T. P. Dzuga, and V. E. Bondybey, *Faraday Disc. Chem. Soc.* **86**, 153 (1988).
- ⁸ R. A. Teichman III, M. Epting, and E. R. Nixon, *J. Chem. Phys.* **68**, 336 (1978); M. A. Epting, M. T. McKenzie, Jr., and E. R. Nixon, *ibid.* **73**, 134 (1980).
- ⁹ R. A. Teichman III and E. R. Nixon, *J. Mol. Spectrosc.* **59**, 299 (1976).
- ¹⁰ S. S. Puri and H. Mohan, *India J. Pure Appl. Phys.* **13**, 206 (1975); S. E. Jonson, D. Cannell, J. Lunacek, and H. P. Broida, *J. Chem. Phys.* **56**, 5723 (1972); H. Sontag and R. J. Weber, *J. Mol. Spectrosc.* **100**, 75 (1983).
- ¹¹ K. A. Gingerich, D. L. Cooke, and F. J. Miller, *J. Chem. Phys.* **64**, 4027 (1976).
- ¹² K. Balasubramanian and K. S. Pitzer, *J. Chem. Phys.* **78**, 321 (1983).
- ¹³ G. Pacchioni, *Mol. Phys.* **55**, 211 (1985).
- ¹⁴ J. Andzelm, N. Russo, and D. R. Salahub, *J. Chem. Phys.* **87**, 6562 (1987).
- ¹⁵ C. S. Feigerle, Ph.D. thesis, University of Colorado, 1983.
- ¹⁶ P. C. Engelking and W. C. Lineberger, *Phys. Rev. A* **19**, 149 (1979).
- ¹⁷ G. Ganteför, M. Gausa, K. H. Meiwes-Broer, and H. O. Lutz, *Z. Phys. D* **12**, 405 (1989).
- ¹⁸ D. G. Leopold, K. K. Murray, A. E. Stevens Miller, and W. C. Lineberger, *J. Chem. Phys.* **83**, 4849 (1985).
- ¹⁹ D. G. Leopold, J. Ho, and W. C. Lineberger, *J. Chem. Phys.* **86**, 1715 (1987).
- ²⁰ J. Ho, K. M. Ervin, and W. C. Lineberger, *J. Chem. Phys.* **93**, 6987 (1990).
- ²¹ H. Hotop and W. C. Lineberger, *J. Phys. Chem. Ref. Data* **14**, 731 (1985).
- ²² C. E. Moore, *Atomic Energy Levels*, Nat. Bur. Stand (U.S.) Circ. No. 467 (1952).
- ²³ K. M. Ervin, J. Ho, and W. C. Lineberger, *J. Chem. Phys.* **91**, 5974 (1989).
- ²⁴ J. Cooper and R. N. Zare, *J. Chem. Phys.* **48**, 942 (1968).
- ²⁵ V. M. Bierbaum, G. B. Ellison, and S. R. Leone, in *Gas Phase Ion Chemistry*, Vol. 3, *Ions and Light*, edited by M. T. Bowers (Academic, New York, 1984), p. 1.
- ²⁶ T. M. Miller, A. E. S. Miller, and W. C. Lineberger, *Phys. Rev. A* **33**, 3558 (1986).
- ²⁷ K. S. Pitzer, *Acc. Chem. Res.* **12**, 271 (1979); K. Balasubramanian, *J. Phys. Chem.* **93**, 6586 (1989).
- ²⁸ (a) C. S. Feigerle, R. R. Corderman, S. V. Bobashev, and W. C. Lineberger, *J. Chem. Phys.* **74**, 1580 (1981); (b) R. R. Corderman, P. C. Engelking, and W. C. Lineberger, *ibid.* **70**, 4474 (1979); (c) P. C. Engelking and W. C. Lineberger, *Phys. Rev. A* **19**, 149 (1979).
- ²⁹ J. L. Hall and M. W. Siegel, *J. Chem. Phys.* **48**, 943 (1968).
- ³⁰ A. Kasdan and W. C. Lineberger, *Phys. Rev. A* **10**, 1658 (1974).
- ³¹ D. Hanstorp, C. Bengtsson, and D. J. Larson, *J. Phys. Rev. A* **40**, 470 (1989).
- ³² V. Radojević, H. P. Kelly, and W. R. Johnson, *Phys. Rev. A* **35**, 2117 (1987).
- ³³ M. K. Gilles, K. M. Ervin, J. Ho, and W. C. Lineberger, *J. Phys. Chem.* (submitted).
- ³⁴ M. L. Polak, J. Ho, G. Gerber, and W. C. Lineberger, *J. Chem. Phys.* **95**, 3046 (1991).
- ³⁵ R. L. DeKock and H. B. Gray, *Chemical Structure and Bonding* (Benjamin, Menlo Park, CA, 1980).
- ³⁶ L.-S. Wang, B. Niu, Y. T. Lee, D. A. Shirley, and K. Balasubramanian, *J. Chem. Phys.* **92**, 899 (1990).